Mid-intensity 30.5 GHz continuous wave exposure of glioblastoma organoids

Palego, Cristiano; Hancock, Chris; Rampazzo, Elena; Persano, Luca; Casciati, Arianna ; Tanori, Mirella; Manusco, Mariateresa; Merla, Caterina

Advanced Concepts and Strategies in Central Nervous System Tumors

Accepted/In press: 01/01/2024

Publisher's PDF, also known as Version of record

Book Chapter Template

Mid-intensity 30.5 GHz continuous wave exposure of glioblastoma organoids

Cristiano Palego, Bangor University, Bangor, United Kingdom, c.palego@bangor.ac.uk
Christopher Hancock, Creo Medical Ltd., Bath, United Kingdom
Elena Rampazzo, University of Padova, Padova, Italy
Luca Persano, University of Padova, Padova, Italy
Arianna Casciati, ENEA, Rome, Italy
Mirella Tanori, ENEA, Rome, Italy
Mariateresa Mancuso, ENEA, Rome, Italy
Caterina Merla, ENEA, Rome, Italy

Abstract

In this chapter, we delve into the therapeutic potential of 30.5 GHz millimetre waves on 3D glioblastoma organoids. We specifically investigated mildly thermal radiation effects in the context of new emerging focused energy deliver and bioelectromagnetic approaches. Our in-house developed exposure system, coupled with a rigorous dosimetry protocol and extensive multi-physics modelling, supported biological endpoints evaluation in terms of transcriptional profiling, cell morphological changes, and cell phenotypic characterization. Crucially, the induced thermal effect was minimal, aligning closely with our simulation models, and indicating the precise control of energy delivery. Notably, a 0.1 W power level enhanced the efficacy of Temozolomide, significantly increasing cell apoptosis while not affecting the differentiation status of glioblastoma organoid cells. This combination suggests a new avenue for glioblastoma treatment, leveraging millimetre wave-induced mechanisms that warrant further investigation. Our findings underscore the promise of this minimally-invasive technique, offering a glimpse into future glioblastoma therapies.

Keywords: continuous waves, dosimetry, energy delivery, glioblastoma organoids, millimetre waves, thermal effect, transcriptomics.

1. Introduction

Glioblastoma multiforme (GBM) remains one of the most aggressive and treatment-resistant forms of brain cancer, with a median survival time of 15 months [1]. Significant breakthroughs in GBM treatment have remained elusive since establishment of the current standard line of treatment – which includes surgery, radiation therapy, and chemotherapy – two decades ago [2].

To overcome these challenges, innovative, energy-based treatment modalities are being explored as alternatives or complements to traditional interventions. These emerging approaches, including Focused Ultrasound (FUS), Tumour-Treating Fields (TTFs), High-Frequency Irreversible Electroporation (H-FIRE), and microwave or millimetre-wave induced hyperthermia, leverage electromagnetic and electromechanical mechanisms to target tumour cells with precision and minimal invasiveness.k

FUS energy delivery can be guided through intraoperative MRI and is being explored as a non-invasive method to manage blood-brain barrier opening (BBBO) and enhance the delivery and effectiveness of chemotherapeutic agents [3]. FUS BBBO also disrupts the immunosuppressive glioblastoma microenvironment potentially aiding in tumour cell detection and initiating an antitumor immune response [4]. Sonodynamic therapy [5] is undergoing a phase 1 clinical trial [6] and uses FUS to make 5-aminolevulinic acid (5-ALA) – a drug designed for visualizing tumours during surgery which is safe for normal brain tissue – cytotoxic to GBM cells in multiple areas of the brain. Histotripsy, a form of cavitation that allows fast mechanical ablation with high-energy ultra-short ultrasound pulses, has shown potential in preclinical models [7].

Tumour-Treating Fields (TTFs) employ low-intensity, intermediate-frequency alternating electric fields to obstruct mitosis selectively in cancer cells [8]. These fields disrupt spindle formation and chromosome segregation for rapidly dividing tumor cells while largely sparing normal tissues. This non-invasive technique has shown promise in clinical trials [9] for newly diagnosed and recurrent glioblastoma, offering a unique mechanism of action that complements traditional therapies.

Other EM approaches aim at cell microenvironment modulation while avoiding direct thermal loading [10-15]. Recent advancements in the use of Pulsed Electric Fields (PEF) for treating brain cancer have focused on their impact on brain cells, including both healthy and cancerous cells. High-Frequency Irreversible Electroporation (H-FIRE), a novel approach employing bipolar electric pulses, has emerged as a promising method for inducing tissue necrosis and cell death while minimizing side effects typically associated with monopolar pulses, such as neuronal stimulation and muscle contraction [10]. The goal is to optimize treatment parameters, particularly for brain tumours like GBM, by achieving effective cell ablation without damaging surrounding healthy tissues.

Research has demonstrated that GBM cells respond to irreversible electroporation or to H-FIRE when exposed to electric fields that exceed a tissue-specific lethal threshold, leading to cell death. This method offers several benefits, including the absence of cytotoxic effects, precise targeting of tumour tissues, a non-thermal ablation mechanism, and preservation of nerves and major blood vessels [11]. Preclinical studies have confirmed the safety and efficacy of these techniques for treating GBM [12]. Interestingly, primary brain tumours containing glioma stem-like cells (GSC) show higher sensitivity to H-FIRE than normal astrocytes, highlighting a potential therapeutic opportunity. However, neuronal stem cells (NSC) exhibit similar sensitivity to these electric pulses, emphasizing the need for personalized cell-specific characterization in clinical applications [13].

H-FIRE has also shown promise as both a monotherapy and in combination with other treatments for malignant glioma. Studies in orthotopic rat models have demonstrated statistically significant improvements in overall survival and increased immune response markers in treated groups compared to controls.

Moreover, H-FIRE at appropriate doses can cause a transient disruption of the BBB, lasting up to 72 hours post-treatment, which may enhance the efficacy of chemotherapy by allowing better drug penetration into the brain [14].

The ability of H-FIRE to selectively ablate cancer stem cells and potentially transform the tumour microenvironment from immunosuppressive to antitumor through Damage Associated Molecular Pattern (DAMP) signalling is particularly exciting. This capability suggests that H-FIRE could be fine-tuned to improve patient outcomes, particularly for those with primary brain tumours, by prolonging overall survival through the targeted destruction of cancer stem cells [15].

While non-thermal EM approaches such as TTFs and H-FIRE offer promising avenues for glioblastoma treatment, other methods intentionally seek to induce thermal stress to achieve therapeutic effects. Among these, microwave ablation has been less researched for brain tumours compared to FUS. This is due to its poorer resolution and the risk of generating heat that can harm surrounding healthy brain tissue, potentially leading to neurological deficits. However, achieving efficient ablation without causing skull heating for off-centre targets remains a challenge even for minimally invasive FUS energy delivery. This issue persists even with hyperthermia [3], where the targeted temperature rise (T_{MAX}=40–45 °C) is lower than for ablation (T_{MAX} >56 °C). Despite these challenges, hyperthermia is a compelling approach due to its role as a potent radio-sensitizer, showing potential to improve treatment outcomes and reduce radiation toxicity. Studies have demonstrated that hyperthermia prior to radiotherapy impairs DNA repair, inhibits survival pathway activation, and reduces glioma stem cell proliferation both *in vitro* and *in vivo* [16, 17].

In this context, exploring mild hyperthermia (ΔT~10 °C, T_{MAX} <35 °C) through Millimetre-Wave (MMW) stimulation is promising. MMW energy delivery is becoming more technologically appealing due to the proliferation of 5G/6G communications and the increasing availability of components. It considerably increases lateral spatial resolution in available electrosurgery tools (e.g., 14.5 GHz [18]) while enabling signal depth of penetration over several cell layers. Additionally, MMW stimulation can potentially elicit or couple with non-thermal dynamics, including absorption dynamics, protein vibration, resonance, unfolding, and hydration [19]. Like other methods that disrupt the tumour microenvironment and generate reactive oxygen species from sono- or radiosensitizers, MMW may offer a unique interaction mechanism and complement other therapeutical approaches. MMW can be delivered to brain tumour by endoscopy yielding limited invasiveness and a focused treatment as required in this terrible pathology [20].

Our study specifically investigates the potential of combining mild temperature increases with chemotherapy, using mid-intensity (P< 5 W) MMW radiation at 30.5 GHz on glioblastoma organoids. These 3D structures, derived from primary patient GBM cells, mimic real tumours' complexity and cellular heterogeneity, reflecting individual tumour variability. We aim to 1) identify the threshold input power density causing stress or modifications in organoids; 2) assess the effects of MMW signals within the mid thermal regime; and 3) explore non-thermal effects in this frequency range. This comprehensive approach successfully highlights cell and molecular responses in a relevant 3D glioblastoma model, advancing the potential of 30.5 GHz MMW as a novel coadjutant treatment option.

2. Material and Methods

2.1 30.5 GHz Source Development

Creo-Medical, UK developed the 30.5 GHz generator in Figure 1 for the present organoid work and potentially supporting future in-vivo MMW stimulation applications. This advanced continuous wave (CW) source comprises a complete millimetre-wave line-up including a mechanically tunable Dielectric Resonator Oscillator (DRO-3404, 30-31 GHz, POUT~11.5 dBm), a pre-amplifier (ERZ-HPA-2000-400-24, Gain=20 dB), and a Power Amplifier (Qorvo's TGA2595-CP). The signal is amplified from the initial 11.5 dBm to an expected 22 dBm after the pre-amplifier, and finally to 36.5 dBm (4.5 W) at the Power Amplifier output.

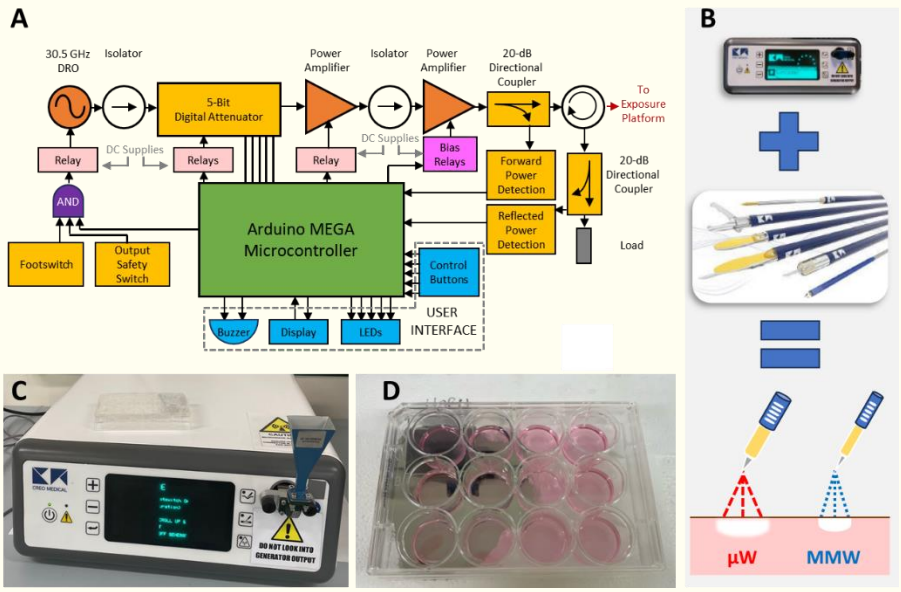

Figure 1: (A): The 30.5 GHz CW source and control unit developed by Creo Medical to support organoid irradiation in this work and **(B):** future minimally invasive MMW procedures with enhanced lateral resolution than in current microwave range settings. **(C):** Closeup view of experimental setup with Ka-band horn antenna and **(D):** the single well container that hosts organoids at its centre and in placed in direct contact of the antenna.

To ensure system integrity and performance, isolators were added to prevent reflected power from damaging sensitive components such as the oscillator and pre-amplifier. Thermal management is achieved by assembling the pre-amplification line-up onto an aluminium plate, which secures each component and acts as a heatsink.

Onboard power supplies and regulation enable the system to operate with only an external mains AC connection (85-250 V), while handling power delivery to each component. The onboard controller automatically sets power supplies and bias conditions for active components. Integrated power detectors support monitoring of forward and reflected power levels, allowing output control via a digital attenuator. Therefore, MMW power attenuation and waveform duration can be entirely managed by the user through an intuitive microcontroller-digital display interface based on an Arduino MEGA, ensuring precise experiment execution and reproducibility.

Housed in its own enclosure, the generator connects to the exposure platform – a Ka-band (26.5-40 GHz) Pasternack PE9850/2F-20 horn antenna – via a quick-release waveguide (WG22). The 30.5 GHz source's power capacity ensures the delivery of sufficient energy at the exposure platform, with its flexible timing control allowing for varied delivery formats in a range of bioelectric experiments.

Two formats were selected for organoid exposure: CW1 (0.1 W Root Mean Square for 20 minutes) and CW2 (0.2 W RMS for 10 minutes). This aimed at comparing different MMW exposure conditions while maintaining the same E=120 J delivered energy. Sham groups were included in the experiments and were exposed in the same setup with no MMW power being delivered.

2.1 Optimization of MMW setup for organoid irradiation

2.1.1 Numerical modelling/optimization approach and optimized setup

The optimal exposure setup for millimetre-wave (MMW) radiation stimulation of glioblastoma organoids was determined through a judicious combination of numerical dosimetry and experimental thermal probing [20]. The key criteria guiding the optimization process were: 1) Impedance matching: quantified by the reflection coefficient (S_{11} scattering parameter), with values at or below -10 dB indicating suitable power transfer; 2) Specific Absorption Rate (SAR) homogeneity: measured by the coefficient of variation (CV), which is the ratio of the standard deviation of the SAR to its mean value over a chosen volume.

Parametric full-wave simulations were conducted using CST Microwave Studio to model the electromagnetic (EM) and thermal behaviour of the setup. Organoids were modelled as dielectric cylinders with a diameter of 2 mm, a height of 0.7 mm, and centres spacing of 5 mm, reflecting experimental conditions. We used complex permittivity values similar to grey matter ($\varepsilon'=20$, $tg\delta=0.3$, [21]) with a slightly different (lower) conductivity. This is justified by the fact that organoid tissue is evidently different from the brain due to the lack of additional heterogeneous cell types and their growth within a culture media that is quite different from the Cerebrospinal Fluid in its composition. The optimized configuration [20] is shown in Figure 2. Using a single 22 mm diameter well in a 12 multi-well plate provided the best balance between transferring MMW power to the samples and minimizing variations in energy absorption across the sample for the well placed in direct contact with the horn antenna. The optimal height of the culture medium in the well was determined to be 3 mm.

2.1.2 Organoid number, impedance matching and SAR inhomogeneity

MMW power transfer is governed by impedance matching between the antenna's output and the sample setup. This involves matching the fundamental Transverse Electric (TE10) mode, launched by the WG22 rectangular waveguide through the horn antenna's flare, with the dielectric properties of the holder/culture/organoid stack. The culture medium, forming the bulk of the sample volume, largely determines the S_{11} response with organoid presence and number exerting a secondary influence.

The number of irradiated organoids n was two, with a spacing of by 5 mm when placed in the holder centre, thus balancing the need for multiple samples with the challenges of culturing a larger number. Critically, the analysis summarized in Figure 2, shows that adding up to n=10 organoids increases their fractional volume (F) to no more than 2%. Therefore, a dielectric mixture model was used to predict the corresponding reflection coefficient degradation would be bound to 0.1 dB, confirming their negligible mismatching impact.

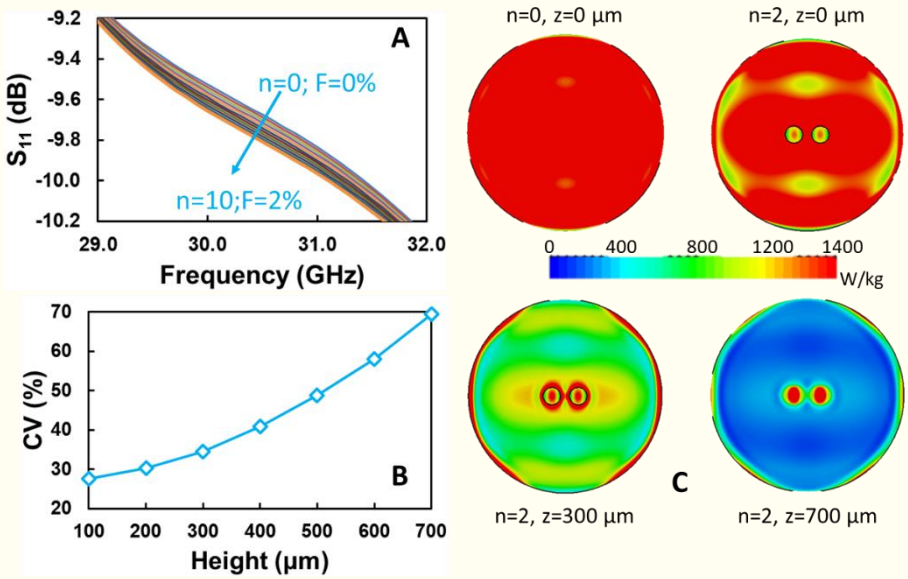

Figure 2: (A): Ka-bad impedance matching response considering dependence from organoid number and fractional volume **(B):** SAR coefficient of variation for organoid slices at different heights along vertical z axis. **(C):** Comparison of SAR distribution for the unloaded medium, and for the medium with two GBM organoids, again at different sampled z heights as from the parametric analysis in [20].

However, Figure 2 also suggests that even this modest effect can cause large variations in energy absorption by different parts of the sample resulting in SAR inhomogeneity. Indeed, the presence of organoids significantly affects the SAR distribution, with substantial variations in homogeneity observed along the height (z-axis) of the organoid due to abrupt changes in electrical properties at the boundaries between the organoids, the culture medium, and the container. The 'meniscus effect' [20] also impacts SAR homogeneity and impedance matching. The curved liquid surface at the well edges increases interface curvature and reduces central medium height, leading to greater organoid fractional volume, thus exacerbating both SAR CV and reflection coefficient degradation.

2.1.3 Thermal modelling and experimental validation

Coupled EM/thermal simulations predicted the temporal evolution of temperature distribution within the sample holder and the organoids. SAR levels in the organoids were evaluated slice by slice at 100 μm intervals. SAR values were averaged over $1mm^3$ cubes to match the sensing volume of thermal probes employed for experiments. These were conducted using a fiber optic probe (Lumasense, US) with two sensors 5mm apart, complemented by thermo-camera imaging for broader area coverage and hotspot characterization.

The SAR(T) dependence was derived by fitting measured temperature curves to the standard bio-heat transfer model for three different power levels and a short (2 s) CW power on-time, which minimizes convective and radiative transfer. This relationship was then extrapolated to longer exposure times and lower power levels, supporting SAR extraction in CW1 and CW2 measurement conditions, both in unloaded media and media containing organoids. To validate our simulation approach, measured and simulated temperature and SAR values without organoids were compared. Measurements and simulations were scaled to a common reference power of 0.5W, revealing only a 10% deviation between predicted and observed values, which fell within the range of measurement standard deviation.

Measured temperature increases (4.5°C for CW1, 7.2°C for CW2) closely matched simulated values (4.4°C and 8.8°C respectively), with thermo-camera results (3.8°C and 9.5°C) providing further confirmation [20]. The higher temperature increase despite shorter exposure time in CW2 suggests that the achieved temperature increase depends more on maximum power (or energy rate) than on exposure time or total delivered energy.

This validated method allowed for fine-tuning of the experimental setup, optimizing parameters such as holder type, holder-antenna distance, and medium height. The final optimized single-well setup, as described in section 2.1.1 (Figure 2), features a 3mm medium height in direct contact with the antenna. Furthermore, this approach enabled parametric studies of Coefficient of Variation (CV) in organoid slices, including centre versus edge effects. The overall procedure was ultimately validated by comparing measured temperature increases (using two independent measurement approaches) with simulated values.

2.1.4 Further optimization results

The validated modelling procedure yielded the results in Figure 2 along with detailed parametric analysis of the exposure setup [20]. We observed highest absorbance at organoid centres, gradually decreasing towards the edges. Nevertheless, SAR coefficient of variation (CV) increased with z peaking at the surface due to dielectric discontinuity at the organoid /medium interface. Interestingly, the SAR pattern with organoids at one height may more closely resemble the distribution without organoids at a different height. This highlights how organoids alter the overall SAR distribution in the well. Along with the previous observation on CV's height dependence, this outlines the complexity of propagation and absorption homogeneity in the investigated multiple medium setting.

This setup provides a foundation for consistent and well-controlled exposure of organoids, supporting future MMW radiation studies. While the impedance matching and SAR CV were fully characterized for the tested two-organoid scenario, this approach can be readily extended to any number of organoids.

2.2 Biological methods

2.2.1 GBM organoid generation and treatment

The primary GBM culture employed within this study was obtained after written informed consent for the donation of tumour tissues under the auspices of the

protocol for the acquisition of human brain tissues obtained from the Ethical Committee of the Padova University-Hospital. Cells were isolated from tumour biopsies taken at surgery according to previously reported protocols [22-23] and cultured in DMEM-F12 supplemented with 10% BIT9500 (StemCell Technologies Inc, Vancouver, Canada), 20ng/ml basic Fibroblast Growth Factor (bFGF) and 20ng/ml Epidermal Growth Factor (EGF; both from Cell Guidance Systems Ltd, Cambridge, UK) in an atmosphere of 2% oxygen, 5% carbon dioxide and balanced nitrogen in a H35 hypoxic cabinet (Don Whitley Scientific Ltd, Shipley, UK) [24].

Organoids were established by embedding 100.000 primary cells (or $1mm^3$-sized tumor fragments) in 10µl Matrigel® (Corning®, Corning, NY) droplets to be polymerized in a standard 37°C incubator. Then freshly generated organoids were cultured in the above-described media in normoxic conditions (21% oxygen) until 21 days before being exposed to specific CW protocols. GBM organoids were routinely monitored for their growth and half-medium changed at least twice a week to ensure their proper growth. After CW exposure, GBM organoids were cultured for additional 24 hours for obtaining transcriptional data, for 72h hours for histological purposes, or treated with 500µM Temozolomide (Selleck Chemicals, Houston, TX) for 5 days before being analyzed for any induction of cell death.

2.2.2 Transcriptional and histological analyses

Transcriptional data of control and CW-exposed organoids were obtained from at least 2 different organoids/experimental replicate after 24 hours from treatment. In particular, after proper extraction (miRNeasy Kit, Qiagen, Hilden, Germany), total RNAs were hybridized to Gene Chip™ WT Clariom™ S arrays (Affymetrix, Santa Clara, CA) according to manufacturer's instructions and analysed as described by using default Affymetrix microarray analysis parameters and normalized by Repeated Measure Analysis (RMA) [20]. Differentially expressed genes between CW-exposed and control organoids were identified using Limma (FDR<0.05 and fold change ≥2).

For histology, control and treated organoids were fixed for 30 minutes in 4% formaldehyde in PBS, washed, and impregnated in 30% sucrose for at least 20 hours before being embedded in Tissue-Tek® O.C.T. Compound (Sakura Finetek USA, Inc., Torrance, CA) and cryosectioned to obtain 10µm thick slides. Hematoxylin and eosin staining was performed according to standard procedures. For immunofluorescence, organoid slides were blocked in 5% BSA (Sigma-Aldrich, St. Louis, MO), 1% goat serum (Vector Laboratories, Newark, CA) PBS solution, and then stained with primary antibodies: Hif-1α (Sigma-Aldrich, Saint Louis, MO) Nestin (Merck, Darmstadt, Germany), βIII-tubulin (Covance Laboratories Inc. Princeton, NJ), S100, Ki67 and GFAP (all from Agilent Dako from Agilent Technologies, Santa Clara, CA); Cleaved-Caspase 3 (Cell Signaling Technology, Danvers, MA).

After incubation with the most appropriate Alexa-dye conjugated secondary antibodies (Thermo Fisher Scientific, Waltham, MA), slides were counterstained with Dapi (Sigma-Aldrich, Saint Louis, MO). For both histology and immunofluorescence, images were collected with a Zeiss Axio Imager M1 epifluorescence microscope (Zeiss, Oberkochen, Germany). Images were analysed and cellular nuclei were counted by the Analyze plugin of ImageJ (https://imagej.nih.gov). Graphs were generated by GraphPad Prism 8.0.1 software

(GraphPad, La Jolla, CA) and data analysed with the included statistical tools. Bar graphs display data arranged as mean ± standard error of the mean (S.E.M.).

3. Results

3.1 Present organoids model of GBM with respect to clinical approaches

GBM is one of the most aggressive and lethal forms of brain cancer, with limited treatment options and a very poor prognosis, as stated in the Introduction. The development of organoid models for GBM has been a significant advancement in the field of cancer research, particularly in studying the disease's biology, drug response, and potential treatment strategies. Here's where current GBM organoid models stand with respect to clinical approaches for: 1) modelling tumour heterogeneity, 2) acting as drug screening tool or support to therapy development, 3) studying tumour microenvironment interactions.

3.1.1 Modelling tumour heterogeneity

For the first point, GBM organoids are excellent at recapitulating the heterogeneity of GBM tumours, including the presence of different cell types, genetic mutations, and microenvironmental features that are critical to the disease. This heterogeneity is often missed in traditional 2D cell cultures but is essential for understanding the complexity of GBM.

This aspect is crucial for the development of personalized medicine, where treatments can be tailored to the specific characteristics of a patient's tumour. The ability to model the patient’s tumour may more accurately help in predicting responses to therapies and in the identification of new therapeutic targets.

3.1.2 Acting as drug screening tool

For the second aspect, GBM organoids offer a platform for high-throughput drug screening, allowing researchers to test a wide range of compounds in a setting that closely mimics the tumour environment. This can lead to the identification of novel drugs or drug combinations that may be effective against GBM. Although still mostly in preclinical stages, this approach has the potential to streamline the drug development process, bringing new therapies to clinical trials faster. Organoids could also help in the development of individualized treatment regimens, potentially improving outcomes by selecting the most effective drugs for each patient.

3.1.3 Studying tumour microenvironment interactions

Finally for the third point, GBM organoids can be co-cultured with other cell types, such as immune cells or cells of the blood-brain barrier, allowing for a more comprehensive study of the tumour microenvironment. This is particularly important in GBM, where interactions between the tumour and its surrounding environment play a crucial role in disease progression and treatment resistance. Insights gained from these studies can inform the development of therapies that

target not just the tumour cells but also the supportive microenvironment, potentially overcoming resistance mechanisms and leading to more effective treatments.

3.1.4 Current clinical integration

GBM organoids are a significant improvement over traditional models, they are still complex and labour-intensive to produce and maintain. Additionally, there can be variability in organoid formation, which might affect the reproducibility of results. Despite their potential, the translation of findings from GBM organoid models to clinical practice is still in its early stages. While organoids provide a more realistic model for studying GBM, clinical trials are needed to validate findings and determine the actual therapeutic benefit in patients. However, there is growing interest in integrating organoid models into clinical workflows, especially for personalized medicine approaches. For example, organoids derived from a patient's tumour could be used to test drug responses ex vivo before administering treatments in vivo, as proposed in our study.

3.2 Proximity of organoid to in-vivo model

3.2.1 GBM organoids well resemble human tumour structure and phenotype.

In order to obtain more reliable *in vitro* models of GBM, able to better resemble the morphological and phenotypic characteristics GBM tumors *in vivo*, we exploited the availability of fresh GBM specimens and further processed them, eventually generating GBM organoids to be subjected to the above selected therapeutic frequencies. To this end, we adapted to our purposes the already available protocols for the generation of cerebral and brain tumour organoids [25-26], allowing the reproducible generation of the GBM organoid models described within this section. In particular, after surgical removal of the tumour, GBM biopsies were mechanically and enzymatically dissociated as previously described [22] to obtain either small sized tumour fragments (≤ $1mm^3$) or single cell suspensions (Figure 3A, panel (i)).

Then, 100.000 GBM cells (or 1 fragment) were dissolved into 10µl of Matrigel and plated onto sterile parafilm molds to allow their polymerization as small droplets/domes (Figure 3A, panel (ii)). After polymerization, these “organoid precursors” were transferred in the culturing media and allowed to grow until being processed for histology and immunofluorescence analyses (Figure 3A, panel (iii)). GBM organoids progressively acquired an increasingly compact morphology, thus achieving their “mature” structure after 20-30 days in culture, eventually resembling the histology of the patient tumour biopsy they were derived from (Figure 3B, C). Accordingly, tumour fragments-generated GBM organoids displayed a similar behaviour, with cancer cells progressively invading the polymerized structure and finally acquiring the same rounded organoid shape and histology, although in a grater timeframe (Figure 3D).

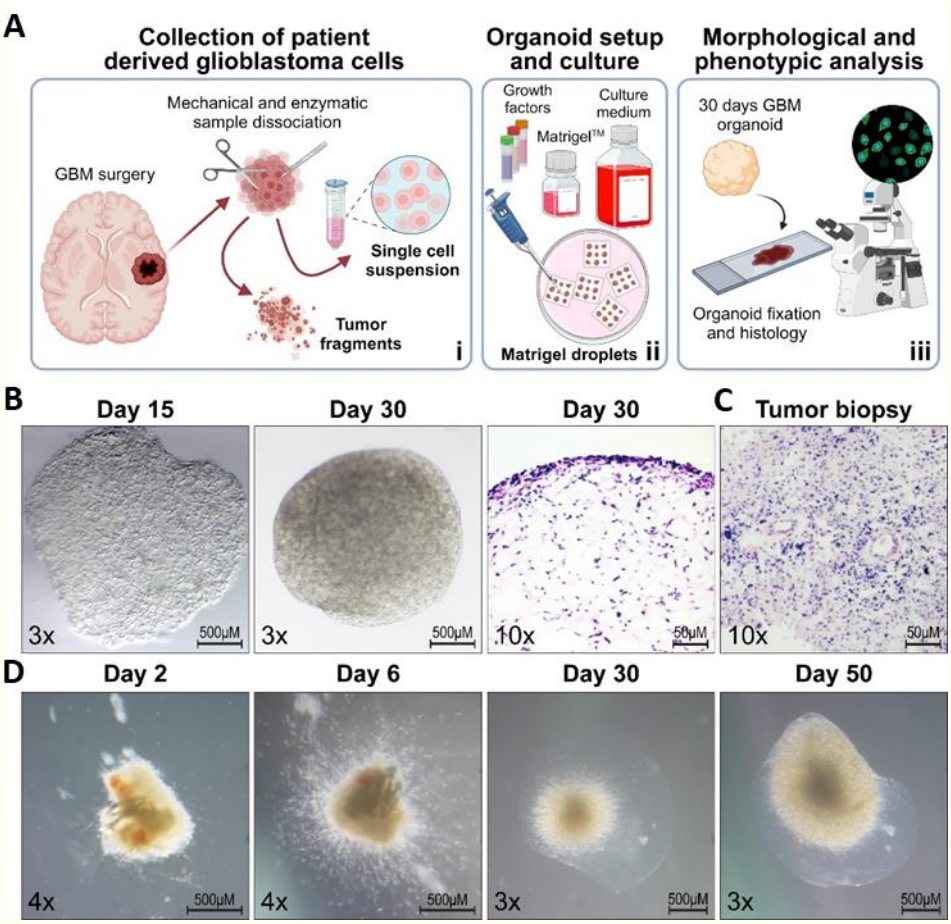

Figure 3: GBM organoid generation and growth. (A): Cartoon summarizing the process of GBM organoid generation and phenotypic characterization, including: i) the collection of human GBM samples from patients and their initial gross processing as minced tissue fragments (diameter ≤ 1mm) and single cell suspensions; ii) GBM organoid preparation and culture by inclusion of cells (10-200x10^3) or fragments into Matrigel® droplets and their subsequent long-term culture in the appropriate supplemented media; iii) GBM organoid fixation, cryosectioning, and histological and immunophenotypic evaluation. Panel (**A**) was created with Biorender.com. **(B, C)**: Representative stereotactic images of GBM organoids during time (day 15-30, **(B)** left panels) and their histological (hematoxylin and eosin staining) characterization (day 30, **(B)** right panel) and comparison with the original tumour tissue GBM cells were derived from **(C)**. **(D)**: Representative stereotactic images of tumour fragments-derived GBM organoid growth during time (day 2-50).

We previously demonstrated that within the GBM mass, phenotypically defined cancer cells are spatially distributed along at least three different layers including a tumour core characterized by necrosis and prominent hypoxia which hosts the most immature and stem-like cell subpopulations, a peripheral layer composed of more differentiated cells (even characterized by a mixed glial-neuronal lineage) and a transition layer between them, characterized by highly proliferating cancer cells [24, 27, 28]. Nevertheless, we should not forget the possible presence of an additional more peripheral layer in which cancer cells invade the normal brain parenchyma, easily recognizable through 5-ALA administration [28]. Interestingly, after 30 days of growth, GBM organoids display a regular rounded shape with a low

cellularized core surrounded by a thick and denser organoid margin (Figure 3B), well resembling human GBM tumours at MRI.

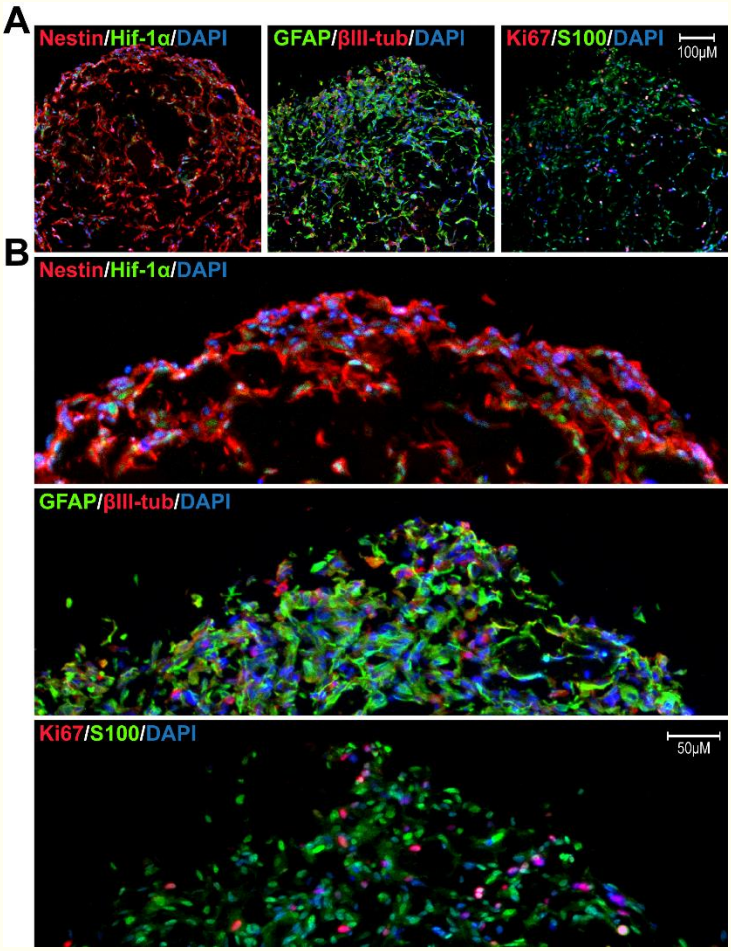

Figure 4. Phenotypic characterization of GBM organoids. Representative immunofluorescence images (**A**, original magnification 10x) and their relative magnification **(B)** showing the spatial expression of a series of GBM phenotypic and proliferation markers, including Nestin (red) and Hif-1α (green), GFAP (green) and β-III-tubulin (red), and Ki67 (red) and S100 (green). Cell nuclei have been counterstained with DAPI (blue).

Phenotypically, GBM organoids are characterized by a heterogenic distribution of different cell phenotypes including: a widespread high expression of the neural stem cell marker Nestin, a higher stabilization of the Hif-1α protein in the inner portions of the organoid [24], a prominent presence of GFAP expressing cells in which are homogeneously distributed cancer cells displaying a mixed neuronal phenotype (e.g. also expressing βIII-tubulin), and a relatively low proliferation index ($Ki67^+$ cells), more compatible with the proliferation rate of GBM cells within human tumors (Figure 4).

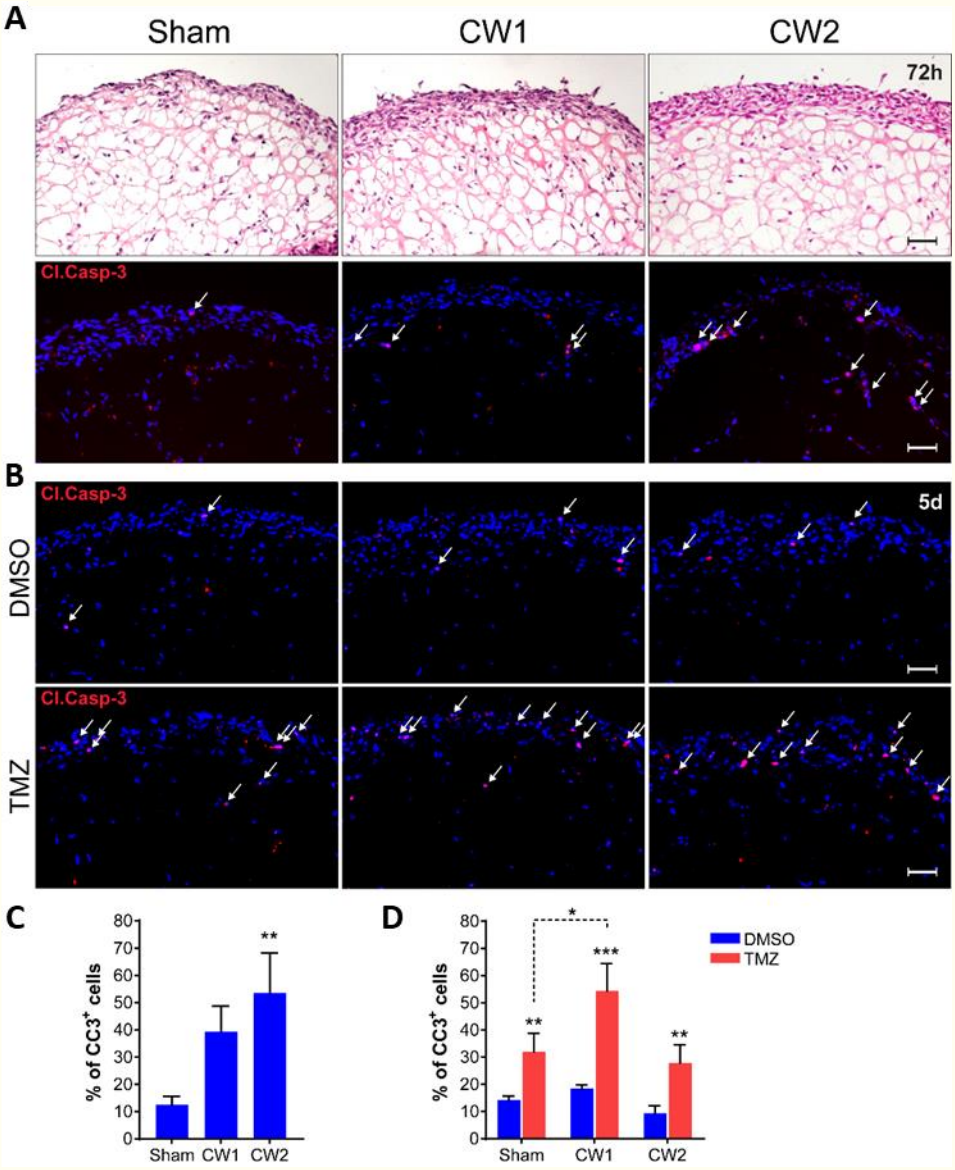

Figure 5. GBM organoid treatment and evaluation of CW effects. (A): Representative haematoxylin and eosin (top) or Cleaved Caspase 3 (Cl.Casp-3, red nuclei indicated by arrows) immunofluorescence (bottom) staining of GBM organoids after 72h from being treated with the sham, CW1, or CW2 exposing protocols. **(B)**: Cleaved Caspase 3 immunofluorescence analysis displaying GBM organoids treated for 5 days with DMSO (top) or TMZ (bottom) both added to the culturing medium 24h from sham or CW1/CW2 exposures. Original magnification: 10x; bar: 50μm. **(C, D)**: Relative quantifications of Cl. Casp-3^+ cells in samples as in A **(C)** and B **(D)**. In **(C)**, *p<0.05, by one-way Anova with Tukey's multiple comparisons test relative to the sham group. In (**D**), asterisks over a column (**p<0.01 and ***p<0.001) indicate a significant difference relative to matched DMSO-treated groups by unpaired t test. Asterisks over brackets (*p<0.05) by one-way Anova with Tukey's multiple comparisons test.

3.2.2 30.5 GHz CW treatment affects GBM cell survival and sensitize organoids to TMZ chemotherapy.

To test *in vitro* the therapeutic efficacy of the simulated CW exposures, a series of 21 days grown organoids were exposed to either CW1 and CW2 treatment protocols or maintained in control conditions before being analysed in terms of transcriptional modulations, histology, and cell death. In particular, after 72h from treatment, CW-exposed organoids did not show any evident variation in size, structure, and histology (Figure 5A). However, immunofluorescence analysis revealed that CW stimulation was sufficient to trigger a pro-apoptotic response of GBM cells residing within the organoids, with CW2 displaying the most severe effects (Figure 5A, C).

In this context, the gene expression profiling of GBM organoids collected after 24 was able to identify 257 differentially expressed genes (DEGs) between sham and CW1 exposed organoids, and 183 DEGs between sham and CW2 exposed organoids. Since the delivered energy was equal in the two different treatments, we aimed to identify the common perturbed genes; by intersecting the two different gene lists we retrieved 143 upregulated - and 22 downregulated genes commonly affected by 30.5 GHz CW exposure. Pathway enrichment analysis through GSEA identified CW-exposed organoids as characterized by an increased expression of genes related to the response to a DNA damage, the activation of DNA repair mechanisms, and cell cycle, with this latter confirmed by a significant expansion of the $Ki67^+$ GBM cell populations within the CW treated organoids [20]. More specifically, the majority of the up-regulated DEGs were related to the regulation of chromatin conformation and replication machinery. While the few down-regulated genes did not significantly enrich for any cellular process. Based on these results, we evaluated the possibility of exploiting the effects displayed by the stimulation with CWs through the combination of a temporally defined chemotherapeutic intervention with TMZ. In particular, we exposed GBM organoids to CWs as described and, after 24 hours, treated them for additional 5 days with TMZ, with the aim of specifically targeting the CW-induced cell proliferation boost. Remarkably, CW pre-treatment dramatically sensitized GBM organoids to TMZ (Figure 5B, D), independently on any transient induction of cell death observed at earlier timepoints (Figure 5C).

3.3 Benefits of mid-intensity thermal sensitization

The MMW irradiation increases the temperature by a few degrees, but this rise remains within the normal temperature range for cells. In fact, their temperature does not exceed 37°C, which is the physiological temperature for cells and tissues. Therefore, the effects observed, as well as their combination with chemotherapeutic agents, cannot simply be attributed to a thermal mechanism similar to that used in hyperthermia applications [20]. In our study, we also noted a stronger effect of TMZ after CW1 exposure, which resulted in a lower temperature increase compared to CW2 exposure, thus supporting our hypothesis. However, the mechanisms underlying the observed effects could be highly complex, and at this point, it is not possible to completely rule out the role of temperature. Clearly, further experiments are necessary to clarify this issue. Nonetheless, the slight temperature increase is beneficial for therapeutic purposes, as it is less invasive and painful for potential future applications in humans.

4. Discussion

The primary objective of this study was to demonstrate the potential of mid-intensity, CW stimulation while determining energy delivery formats that yield significant end-points in a glioblastoma organoid model. Our findings not only achieved this goal but also outlined the need for further investigation in this field.

The extinguishing effect of CW stimulation when cells are not re-exposed could not be within the scope of the present study. This limitation was not solely due to time constraints but also stemmed from the uncertainty surrounding the number of repeated stimulations organoids can undergo while still providing meaningful results. Future research should rely on additional cell biology experiments aimed at elucidating this aspect by implementing a rigorous evaluation of several close-range experimental timepoints within the proposed actionable timeframe as it could significantly impact the design of therapeutic protocols. Nevertheless, this will need dedicated efforts and time.

Our results showed that CW2 induced more pronounced apoptosis and less proliferation in the mid-term range (72 hours after exposure), likely due to the milder temperature increase compared to CW1, which delivers higher power. Consequently, the CW/TMZ combination more effectively induced apoptosis for the CW1 protocol, as CW1 favors proliferation, which is then targeted by TMZ. These observations underscore the complex interplay between CW parameters, cellular responses, and chemotherapeutic efficacy. Identifying the optimal window for TMZ administration post-exposure, along with fine-tuning signal intensity and exposure duration, could lead to an enhanced chemotherapeutic response for TMZ or other alkylating agents.

While our focus on TMZ provided valuable insights, future studies should expand the scope to include different chemotherapeutic drugs with diverse mechanisms of action. Moving beyond agents that directly affect proliferating cells could offer a more comprehensive understanding of how CW stimulation interacts with various treatment modalities targeting cancer cell migration and infiltration, rather than proliferation. Future studies could explore the effects of CW stimulation combined with matrix metalloproteinase inhibitors, which impede tumor invasion, or anti-angiogenic agents that restrict tumor vascularization. Additionally, examining the interaction between CW exposure and immunomodulatory therapies could unveil potential synergies in activating anti-tumor immune responses. These diverse approaches may uncover unexpected therapeutic opportunities and provide a more holistic strategy for combating the complex nature of GBM.

Conclusion(s)

In summary, we comprehensively characterized an exposure setup for 30.5 GHz CW suitable for experiments on 3D GBM organoids, in terms of numerical/experimental dosimetry and thermal regimen. From our characterization, we demonstrated the possibility to use this exposure modality (especially CW1 protocol) as a therapeutic adjuvant in a future possible treatment for GBM. Our approach impacts the functioning and behaviour of GBM cells by inducing a statistically significant increase of proliferation, as confirmed by both transcriptional and functional analyses. This result leads to the enhancement of a

subsequent TMZ administration and to future and innovative combination therapies for GBM.

While the present study did not demonstrate direct MMW radiation-induced cell differentiation pathways, the growing body of literature on EM-based microenvironment manipulation suggests promising avenues for future research. These emerging approaches may lead to the development of therapeutic modalities that selectively target GBM cancer stem cells, potentially increasing their susceptibility to conventional treatments and addressing one of the major challenges in GBM therapy.

Acknowledgments

The authors gratefully acknowledge the support from Bangor University's School of Computer Science and Engineering for the open access publication of this contribution. The work in this chapter was supported by Project ECS 0000024 Rome Technopole, -CUP B83C22002820006, NRP Mission 4 Component 2 Investment 1.5, Funded by the European Union -NextGenerationEU. This work was also supported by CARIPARO Foundation project number 20/16.

Conflict of Interest

CH was employed by Creo Medical Limited. The remaining authors declare no conflict of interest.

Notes/Thanks/Other declarations

Place any other declarations, such as "Notes", "Thanks", etc. in before the References section. Assign the appropriate heading.

References

[1] Rong L, Li N, Zhang Z. Emerging therapies for glioblastoma: current state and future directions. Journal of Experimental & Clinical Cancer Research. 2022;41(1):142. DOI: 10.1186/s13046-022-02349-7

[2] Stupp R, Mason WP, van den Bent MJ, Weller M, Fisher B, Taphoorn MJ, Belanger K, Brandes AA, Marosi C, Bogdahn U, Curschmann J, Janzer RC, Ludwin SK, Gorlia T, Allgeier A, Lacombe D, Cairncross JG, Eisenhauer E, Mirimanoff RO. Radiotherapy plus concomitant and adjuvant temozolomide for glioblastoma. *New England Journal of Medicine*. 2005;352:987-996. DOI: 10.1056/NEJMoa043330

[3] Meng Y, Hynynen K, Lipsman N. Applications of focused ultrasound in the brain: from thermoablation to drug delivery. *Nature Reviews Neurology*. 2021;17:7-22. DOI: 10.1038/s41582-020-00418-z

[4] Aldape K, Brindle KM, Chesler L, Chopra R, Gajjar A, Gilbert MR, Gottardo N, Gutmann DH, Hargrave D, Holland EC, Jones DTW, Joyce JA, Kearns P, Kieran MW, Mellinghoff IK, Merchant M, Pfister SM, Pollard SM, Ramaswamy V, Rich JN, Robinson GW, Rowitch DH, Sampson JH, Taylor MD, Workman P, Gilbertson RJ. Challenges to curing primary brain tumours. Nature Reviews Clinical Oncology. 2019;16(8):509-520. DOI: 10.1038/s41571-019-0177-5

[5] Bonosi L, Marino S, Benigno UE, Musso S, Buscemi F, Giardina K, Gerardi R, Brunasso L, Costanzo R, Iacopino DG, Maugeri R. Sonodynamic therapy and magnetic resonance-guided focused ultrasound: new therapeutic strategy in glioblastoma. *Journal of Neuro-Oncology*. 2023;163:219-238. DOI: 10.1007/s11060-023-04333-3

[6] https://clinicaltrials.gov/study/NCT06039709?term= shayan% 20moosa& rank=1

[7] Roberts, J.W., Powlovich, L., Sheybani, N., LeBlang, S. Focused ultrasound for the treatment of glioblastoma. Journal of Neuro-Oncology. 2022;157:237-247. DOI: 10.1007/s11060-022-03974-01

[8] Carrieri FA, Smack C, Siddiqui I, Kleinberg LR, Tran PT. Tumor treating fields: at the crossroads between physics and biology for cancer treatment. Frontiers in Oncology. 2020;10:575992. DOI: 10.3389/fonc.2020.575992

[9] Shah PP, White T, Khalafallah AM, Romo CG, Price C, Mukherjee D. A systematic review of tumor treating fields therapy for high-grade gliomas. Journal of Neuro-Oncology. 2020;148:433-443. DOI: 10.1007/s11060-020-03563-z

[10] Campelo SN, Popelka S, Anderson RS. Structure of protein-surface interaction layers in polymer brushes. APL Bioengineering. 2023;8:026117. DOI: 10.1063/j.0198382

[11] Lorenzo MF, Arena CB, Davalos RF, Maximizing local access to therapeutic delivery in Glioblastoma. Part III: Irreversible electroporation and High-frequency Irreversible electroporation for the eradication of Glioblastoma. In: Codon Publications, editors. Glioblastoma. 1st ed. Brisbane: Codon Publications; 2017. p. 19. DOI: 10.15586/codon.glioblastoma.2017

[12] Murphy KR, Rogers A, Pavlovic D. Bioelectrochemistry and biophysical analysis of cell interaction. Bioelectrochemistry. 2022;144:108001. DOI: 10.1016/j.bioelechem.2021.108001

[13] Ivey JW, Wasson EM, Alinezhadbalalami N, Kanitkar A, Debinski W, Sheng Z, Davalos RF, Verbridge SS. Characterization of Ablation Thresholds for 3D-Cultured Patient-Derived Glioma Stem Cells in Response to High-Frequency Irreversible Electroporation. Research (Wash D C). 2019; 2019:8081315. DOI: 10.34133/2019/8081315

[14] Campelo SN, Popelka S, Kim BS. Advances in cancer immunotherapy. Frontiers in Oncology. 2023;13:1171278. DOI: 103389/fonc.2023.1171278

[15] Partridge B, Long CJ, Hainline B. Neuromodulation techniques in behavioral neuroscience. Journal of Neuroscience Methods. 2020;330:108630. DOI: 10.1016/j.jneumeth.2020.108630

[16] Frey B, Weiss E-M, Rubner Y, Wunderlich R, Ott OJ, Sauer R, Fietkau R, Gaipl US. Old and new facts about hyperthermia-induced modulations of the immune system. International Journal of Hyperthermia. 2012;28(6):528-542. DOI: 10.3109/02656736.2012.677933.

[17] Zhu L, Altman MB, Laszlo A, Straube W, Zoberi I, Hallahan DE, Chen H. Ultrasound hyperthermia technology for radiosensitization. Ultrasound in Medicine & Biology. 2019;45(5):1025-1043. DOI: 10.1016/j.ultrasmedbio.2018.12.007

[18] Hancock CP, Chaudhry S, Wall P, Goodman AM. Proof of concept percutaneous treatment system to enable fast and finely controlled ablation of biological tissue. Medical & Biological Engineering & Computing. 2007;45(6):531-540. DOI: 10.1007/s11517-007-0184-z

[19] Sugiyama, J.-I., Tokunaga, Y., Hishida, M., Tanaka, M., Takeuchi, K., Satho, D., Imashimizu, M. Nonthermal acceleration of protein hydration by sub-terahertz irradiation. Nature Communications. 2023;14:2825. DOI: 10.1038/s41467-023-38462-0

[20] Rampazzo E, Persano L, Karim N, Hodgking G, Pinto R, Casciati A, Tanori M, Zambotti A, Bresolin S, Cani A, Pannicelli A, Davies IW, Hancock C, Palego C, Viola G,

Mancuso M, Merla C. On the effects of 30.5 GHz sinusoidal wave exposure on glioblastoma organoids. Frontiers in Oncology. 2024;14:1307516. DOI: 10.3389/fonc.2024.1307516

[21] https://itis.swiss/virtual-population/tissue-properties/database/

[22] Pistollato, F., Persano, L., Della Puppa, A., Rampazzo, E., Basso, G. Isolation and expansion of regionally defined human glioblastoma cells in vitro. Current Protocols in Stem Cell Biology. 2011 May;Chapter 3:Unit 3.4. DOI: 10.1002/9780470151808.sc0304s172.

[23] Porcù, E., Maule, F., Manfreda, L., Mariotto, E., Bresolin, S., Cani, A., Bortolozzi, R., Della Puppa, A., Corallo, D., Viola, G., Rampazzo, E., Persano, L. Identification of Homoharringtonine as a potent inhibitor of glioblastoma cell proliferation and migration. Translational Research. 2023 Jan;251:41-53. DOI: 10.1016/j.trsl.2022.06.0173.

[24] Pistollato, F., Abbadi, S., Rampazzo, E., Persano, L., Della Puppa, A., Frasson, C., Sarto, E., Scienza, R., D'avella, D., Basso, G. Intratumoral hypoxic gradient drives stem cells distribution and MGMT expression in glioblastoma. Stem Cells. 2010 May;28(5):851-62. DOI: 10.1002/stem.4152.

[25] Lancaster, M.A., Knoblich, J.A. Generation of cerebral organoids from human pluripotent stem cells. Nature Protocols. 2014 Oct;9(10):2329-40. DOI: 10.1038/nprot.2014.158.

[26] Hubert, C.G., Rivera, M., Spangler, L.C., Wu, Q., Mack, S.C., Prager, B.C., Couce, M., McLendon, R.E., Sloan, A.E., Rich, J.N. A Three-Dimensional Organoid Culture System Derived from Human Glioblastomas Recapitulates the Hypoxic Gradients and Cancer Stem Cell Heterogeneity of Tumors Found In Vivo. Cancer Research. 2016 Apr 15;76(8):2465-77. DOI: 10.1158/0008-5472.CAN-15-2402.

[27] Persano, L., Rampazzo, E., Della Puppa, A., Pistollato, F., Basso, G. The three-layer concentric model of glioblastoma: cancer stem cells, microenvironmental regulation, and therapeutic implications. ScientificWorldJournal. 2011;11:1829-41. DOI: 10.1100/2011/736480.

[28] Della Puppa, A., Persano, L., Masi, G., Rampazzo, E., Sinigaglia, A., Pistollato, F., Denaro, L., Barzon, L., Palù, G., Basso, G., Scienza, R., d'Avella, D. MGMT expression and promoter methylation status may depend on the site of surgical sample collection within glioblastoma: a possible pitfall in stratification of patients? Journal of Neuro-Oncology. 2012 Jan;106(1):33-41. DOI: 10.1007/s11060-011-0639-9.

[29] Rampazzo, E., Della Puppa, A., Frasson, C., Battilana, G., Bianco, S., Scienza, R., Basso, G., Persano, L. Phenotypic and functional characterization of Glioblastoma cancer stem cells identified through 5-aminolevulinic acid-assisted surgery [corrected]. Journal of Neuro-Oncology. 2014 Feb;116(3):505-13. DOI: 10.1007/s11060-013-1348-3.